Acid-Functionalized Polysilsesquioxane—Nafion Composite Membranes with High Proton Conductivity and Enhanced Selectivity

Kui Xu, Chalatorn Chanthad, Matthew R. Gadinski, Michael A. Hickner, and Qing Wang*

Department of Materials Science and Engineering, The Pennsylvania State University, University Park, Pennsylvania 16802

ABSTRACT A series of new Nafion-based composite membranes have been prepared via an in situ sol-gel reaction of 3-(trihydroxylsilyl)propane-1-sulfonic acid and solution casting method. The morphological structure, ion-exchange capacity, water uptake, proton conductivity, and methanol permeability of the resulting composite membranes have been extensively investigated as functions of the content of sulfopropylated polysilsesquioxane filler, temperature, and relative humidity. Unlike the conventional Nafion/silica composites, the prepared membranes exhibit an increased water uptake and associated enhancement in proton conductivity compared to unmodified Nafion. In particular, considerably high proton conductivities at 80 and 120 °C under 30% relative humidity have been demonstrated in the composite membranes, which are over 2 times greater than that of Nafion. In addition to a remarkable improvement in proton conductivity, the composite membranes display lower methanol permeability and superior electrochemical selectivities in comparison to the pure Nafion membrane. These unique properties could be exclusively credited to the presence of pendant sulfonic acid groups in the filler, which provides fairly continuous proton-conducting pathways between filler and matrix in the composite membranes and thus facilitates the proton transport without the anticipated trade-off between conductivity and selectivity. This work opens new opportunities of tailoring the properties of Nafion—the benchmark fuel cell membrane—to obviate its limitations and enhance the conductive properties at high temperature/low humidity and in direct methanol fuel cells.

KEYWORDS: composite materials • polymeric materials • fuel cells • proton conductivity • selectivity

1. INTRODUCTION

Proton exchange membrane fuel cells (PEMFCs) have received considerable attention as clean and efficient power sources for automotive, stationary, and portable applications (1, 2). Perfluorosulfonated ionomers represented by Nafion are typically used as electrolytes that facilitate proton transport from the anode to the cathode in PEMFCs (3—5). The combination of a robust tetrafluoroethylene backbone with acidic perfluorosulfonic acid side chains renders outstanding chemical, thermal, and mechanical stability and high proton conductivity at moderate temperatures (≤80 °C) and 100% relative humidity (RH). However, such membranes tend to dehydrate significantly at high temperature and/or low humidity, resulting in a radical loss of proton conductivity and, in most cases, irreversible phase transformation or destruction of the membranes (6, 7). Operation of PEMFCs at high temperatures provides a number of technological benefits, including acceleration of the electrode reactions, improved tolerance to impurities in the fuel gas, and simplified water and thermal management (8, 9).

To this end, it has been attempted to modify Nafion with nanoparticles of hygroscopic oxides such as silica, titania, and zirconia phosphate (10—15). It is envisioned that introduction of these hydrophilic additives in the polymer increases the hydration of the membrane and reduces the evaporation of water. The enhanced water absorbability from the hydrophilic oxides enables low humidification and high-temperature operation of PEMFCs. The fuel crossover, e.g. methanol in direct methanol fuel cells (DMFCs), is also strongly suppressed through impregnating the membranes with inorganic particles (16—18). The high methanol permeability of Nafion leads to significant losses in fuel cell power density and efficiency and thereby impedes the widespread commercial use of DMFCs (19). However, the composite approach does not always present distinctive advantages in fuel cell performance, mainly because the excessive addition of these less conductive fillers results in proton conductivities lower than that of pristine Nafion (20—22). Incorporating heteropolyacid proton conductors, such as phosphotungstic acid (PTA) and silicotungstic acid (SiWA), into Nafion-based composites provides water-independent ionic conduction and achieves better PEMFC performance at high temperature and low humidity (23, 24). A profound drawback of this method is that the operational lifetime is limited by the leaching of the free acid from the membrane in the presence of liquid water at elevated temperatures, which causes a drop in conductivity of many orders of magnitude during fuel cell operation. Therefore, Nafion doped with fillers containing chemically tethered proton conducting groups

* To whom correspondence should be addressed. E-mail: wang@matse.psu.edu.
Received for review July 26, 2009 and accepted October 16, 2009

DOI: 10.1021/am900498u

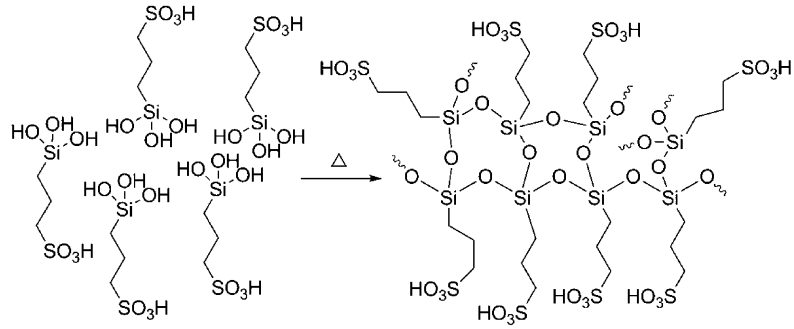

FIGURE 1. Chemical structure and sol-gel reaction of 3-(trihydroxylsilyl)propane-1-sulfonic acid.

would be highly desirable. For instance, composite membranes have been prepared with acid-functionalized additives such as sulfonated montmorillonite, sulfonated titanate, and superacid zirconia (25, 26). Nonhomogeneous dispersion of dopants is usually found in this manner because of unavoidable particle agglomeration. Sulfonated phenethylsilica has been incorporated into Nafion to improve its proton conductivity and water uptake characteristics (27). Substantially increased proton conductivity at 80 °C and 100% RH was observed in comparison to a Nafion matrix. Sulfonated mesoporous silica has also been introduced into Nafion by the sol-gel process of silica precursors followed by postoxidation reactions to generate sulfonic acid moieties, whereas there is some uncertainty about the concentration of the acid groups (28−31).

Herein, we report novel Nafion-based composite membranes fabricated by the in situ sol-gel reaction of 3-(trihydroxylsilyl)propane-1-sulfonic acid (THSPSA) (32) and the solution casting method. THSPSA was chosen as the oxide precursor due to its multifunctional structure, as shown in Figure 1. The hydrophilic nature of THSPSA ensures the compatibility between the inorganic phases and the ionic domains of the Nafion matrix and hence improves the homogeneity of composite membranes. In addition, the resulting sulfopropylated polysilsesquioxane (SiOPS) allows for continuity of proton conduction between the fillers and Nafion through the covalently attached alkyl sulfonic acids. The remarkable utility of the prepared composite membranes at elevated temperatures and low humidity has been demonstrated. Unlike the conventional Nafion/silica composites, the prepared membranes exhibit high methanol resistance without the anticipated trade-off between reduced methanol permeability and decreased proton conductivity in DMFCs.

2. EXPERIMENTAL SECTION

Materials. 3-(Trihydroxylsilyl)propane-1-sulfonic acid (THSPSA) (35 wt % in water) was purchased from Gelest. Inc. Nafion raw solution (5 wt %) in water/alcohol and other chemicals were purchased from Sigma-Aldrich. All chemicals were used as received without any further purification.

Membrane Preparation. A DMF solution of Nafion was prepared by evaporation of Nafion raw solution in air at room temperature until solid resin was obtained, followed by redissolving in DMF. Measured amounts of THSPSA aqueous solution (35 wt %) and Nafion/DMF solution (15 wt %) were then mixed and magnetically stirred at room temperature for 6 h to ensure complete mixing. The resulting solution was casted onto a glass plate and heated to 55 °C for 2 h, 75 °C for 4 h, and 100 °C for 6 h. Afterwards, the obtained solid membrane was placed in a vacuum oven at 150 °C for 12 h to remove any residual solvent and to be annealed. The amounts of THSPSA and Nafion/DMF solution were varied to obtain composites with different filler loadings. The resulting membranes were treated before use by boiling them in 1 M H_2SO_4 solution for 0.5 h, rinsing with deionized (DI) water, boiling in DI water for 0.5 h, and then rinsing again with DI water until pH 7. The typical thickness of the membranes at full hydration falls within the range of 65−85 μm.

Structural Characterization. FTIR spectra of the composite membranes were recorded on a Varian Digilab FTS-800 spectrometer with a resolution of 2 cm^{-1}. The thermogravimetric analysis (TGA) measurement was performed on a TA Instruments Model 2950 at a heating rate of 20 °C/min under N_2 from room temperature up to a maximum of 800 °C. Transmission scanning microscopy (TEM) images were taken on a JEOL JEM-1200 EX II TEM. In order to enhance the contrast, the membranes were stained by lead acetate, embedded in epoxy resin, and cured overnight in an oven at 60 °C. The samples were then sectioned by microtome to yield 100 nm slices and placed on copper grids before TEM viewing. Low-temperature dynamic scanning calorimetry (DSC) measurements were performed to characterize the water state in hydrated membranes. Fully hydrated membrane samples (~15 mg) were blotted with a lab wipe to remove surface water and then instantly placed into a DSC pan (O-ring model-TA Instruments) and sealed. The sample was immediately put in the calorimeter and cooled to −80 °C. In a typical run, after being held at −80 °C for 20 min, the samples were heated to 100 °C at a heating rate of 5 °C/min. The heat of fusion for the water in the membranes was computed using eq 1:

$$\Delta H_f = H/W_{H2O} \quad (1)$$

where ΔH_f is the heat of fusion for the water contained in the sample, W_{H2O} is the weight of water in the sample, and H is the integrated energy from the melting endotherm.

Water Uptake, Ion-Exchange Capacity, and Hydration Number. Membranes were dried under vacuum over at 70 °C for at least 4 h and cooled to room temperature in a desiccator. Their masses in the "dry" state, W_{dry}, were measured. Then the membranes were immersed in DI water at a set temperature for 2 h. After removal of the surface water, the mass in the "wet" state, W_{wet}, was measured. The water uptake was calculated according to eq 2:

$$\text{water uptake} = \frac{W_{wet} - W_{dry}}{W_{dry}} \times 100\% \quad (2)$$

The ion exchange capacity (IEC) of the membrane was determined by the titration technique as detailed in ref 42. The hydration number λ was calculated from IEC, water uptake and molecular weight of water ($M_{w,H2O}$) as given in eq 3.

$$\lambda = \frac{\text{water uptake}}{M_{w,H2O} \times \text{IEC}} \quad (3)$$

Proton Conductivity and Methanol Permeability. In-plane proton conductivity (σ) of the membranes was measured by the electrochemical impedance spectroscopy (EIS) technique. Impedance data were acquired using a Solartron 1260 gain phase analyzer over the frequency range of 1 Hz to 100 kHz. Conductivity measurements under fully hydrated conditions were performed when the samples were equilibrated in water at various temperatures. The measured temperature was varied from 30 to 80 °C. Proton conductivity was also measured under different temperature and humidity conditions. The humidity at 30 and 80 °C was controlled by an ESPEC SH240 environmental chamber. The proton conductivity measurement at 120 °C was performed on a hook-up of BT-112 conductivity cell and humidification system provided by BekkTech LLC under an air flow rate of 500 sccm. The samples were tested as follows: (1) conditioned at set temperatures and 90% RH for 2 h and (2) stepped from 90% to 30% RH at 10% RH intervals, allowing 20−30 min of stabilization at each RH. The conductivity was calculated using eq 4:

$$\sigma = \frac{L}{R \times T \times W} \quad (4)$$

where L is the distance between two electrodes, T and W are the thickness and width of the membranes, respectively, and R is the membrane resistance determined from AC impedance spectra.

Methanol permeability was determined in a standard membrane-separated diffusion cell (35). A glass cell containing methanol aqueous solution and DI water in two identical compartments separated by the test membrane was utilized for permeability measurements. The membranes were placed between the two compartments by a screw clamp. Both compartments were magnetically stirred during the permeation experiments. The concentration of methanol was quantified using a differential refractometer. Methanol permeability was calculated from the slope of the straight-line plot of methanol concentration versus permeation time.

3. RESULTS AND DISCUSSION

As illustrated in Figure 2, a series of the composite membranes containing 4, 8, 12, 16, and 20 wt % THSPSA were obtained by drying the mixture of Nafion DMF solution (15 wt %) and THSPSA aqueous solution (35 wt %) and denoted as NSS-4, -8, -12, -16, and -20, respectively. Nafion recast membrane (NSS-0) was also prepared using the same procedure for comparison. It was observed that the composite membranes maintain excellent mechanical properties and crack-free quality even when the inorganic phase loading reaches 30 wt %. The formation of polysilsesquioxane in the composites was confirmed by the FTIR spectra, as shown in Figure 3. The characteristic vibrational bands appear at 801, 995, and 1028 cm^{-1}, indicative of the Si−O−Si bonds (33). Furthermore, these Si−O−Si symmetric and asymmetric stretching peaks become more intense with the amount of THSPAS incorporated. The absorption band of S−O stretching from $-SO_3H$ groups at 1125 cm^{-1} overlaps with the broad band from 1100 to 1300 cm^{-1} assigned to C−F stretching from Nafion. The existence of a weak Si−OH band at 890 cm^{-1} suggests an incomplete condensation of the sol-gel process, presumably due to the steric hindrance of the alkyl chain and Coulombic repulsion between the protonated THSPSA. TGA curves indicate that the composite and Nafion membranes have similar onset temperatures around 315−325 °C corresponding to the degradation of sulfonic acid groups in the side chains. Morphological structures in the composite membranes were examined by TEM. Although it is impossible to directly observe hydrated membranes using this technique, TEM results are still valuable in offering some insights on the ordering and size of ionic domains in membranes. Figure 4 shows TEM images of the membranes stained with lead acetate, in which the dark regions correspond to the aggregation of sulfonic acid groups both from SiOPS and Nafion and the white areas are associated with the hydrophobic regions of Nafion. Phase-separated morphologies with compositional heterogeneity on the scale of 5−10 nm can be clearly seen in the composites, similar to those in unmodified Nafion. This is consistent with the speculation that the morphology of Nafion acts as a template for the sol-gel reaction of THSPSA in the ionic domains of Nafion matrix (34). As the THSPSA content increases, hydrophilic agglomerates with diameters ranging from 20−40 nm emerge in the TEM images, which can be ascribed to the formation of large SiOPS nanostructures that grow out of the polar domain of Nafion and become entangled throughout the matrix. These SiOPS aggregates are distributed relatively uniformly in the composite membranes, as verified in the lower magnification TEM images.

IECs of the membranes measured by titration with 0.1 M NaOH are given in Table 1. The IEC was found to increase rapidly from 0.92 mmol/g of NNS-0 to 1.25 mmol/g of NNS-12. A further increase of THSPSA content from 12 to 20 wt % does not lead to an obvious rise in IEC. It should be noted that the water uptake of the composite membranes follows the same trend. As shown in Table 1, a gradual increase in water uptake from 19.4 to 28.7% is observed with increasing the THSPSA concentration up to 12 wt %, and the water uptake levels off thereafter. The saturation of IEC and water uptake can be rationalized in terms of the large SiOPS nanoclusters formed at high precursor concentrations, which trap the inside sulfonic acid groups and make them not easily accessible for interactions with water and Na^+/H^+ exchange. Analogous to water uptake, the average number of water molecules per sulfonic acid group, λ, of the composites is also strongly dependent on IEC. It can be seen from Table 1 that λ increases steadily from 11.7 for NSS-0 to 12.8 for NSS-12 and then slowly to 13.1 for NSS-20, owing

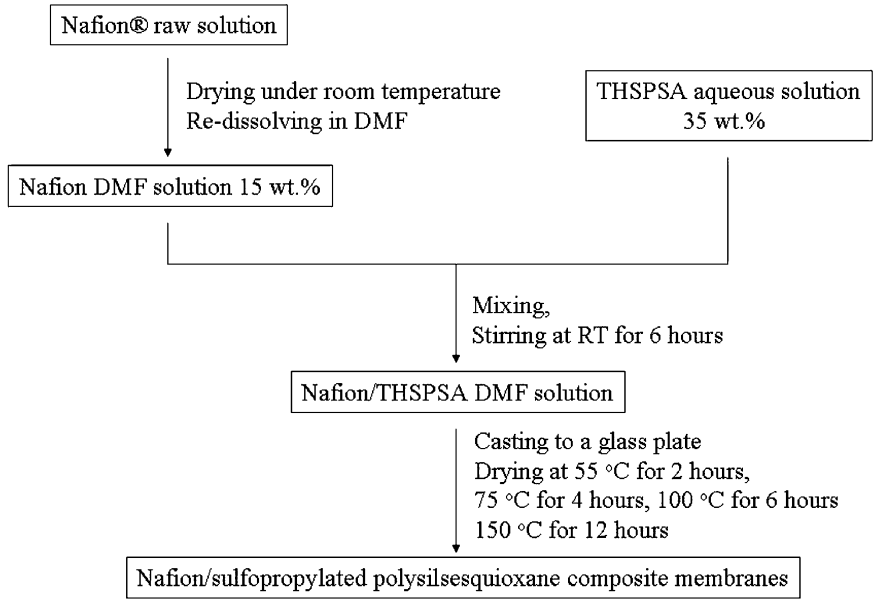

FIGURE 2. Preparation procedure of Nafion/sulfopropylated polysilsesquioxane composite membranes.

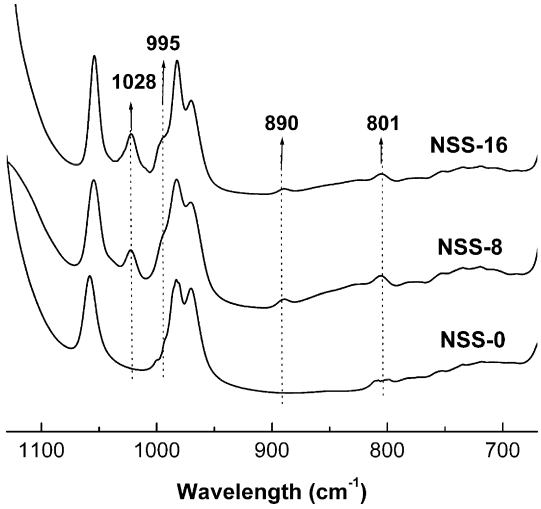

FIGURE 3. FT-IR spectra of the composite membranes.

to a greater number of the sulfonic acids introduced by THSPSA. λ is one of the basic parameters implying that the membranes can be effectively hydrated for sulfonic acid groups, which is essential to proton conduction. To probe the state of water inside the hydrated membranes, ΔH_f for water has been measured using low-temperature DSC (35). In general, a large value of ΔH_f for water represents a high concentration of unbound and weakly bound water, since the water molecules that are strongly bound to ionic groups do not contribute to the melting endotherm in the DSC curves (36). It is believed that the interconnected channels between ionic domains in Nafion are formed by interfacial water, which is only loosely bound to the membranes and play a crucial role in proton conduction (37, 38). In comparison to pure Nafion recasting membrane (NSS-0), it is evident that the composite membranes, especially in the cases of NSS-4 and NSS-8, contains more weakly bound and free water, which could be correlated to higher concentration of sulfonated groups that interact with water molecules through hydrogen bonding.

Table 2 summarizes the proton conductivity of the membranes measured at 30 °C and fully hydrated state. In comparison with pristine Nafion, the composites exhibit improved proton conductivity, resulting from the increased IEC and water uptake values. The conductivity increases progressively with the THSPSA content and becomes steady at ~0.101 S/cm for NSS-16 and NSS-20, which is in accordance with the IEC and water uptake trends presented in Table 1. For purposes of comparison, we have also prepared Nafion/silica composites using the sol-gel reaction of tetraethoxylsilane (TEOS). The proton conductivities measured at 30 °C under fully hydrated conditions are 0.071 S/cm for a 5 wt % TEOS membrane and 0.07 S/cm for a 15 wt % TEOS membrane. These values are in close agreement with the conductivities previously reported in the literature (39) and are lower than that of unfilled Nafion having a conductivity of 0.084 S/cm. The dependence of the proton conductivity of the membranes on humidity and temperature is illustrated in parts a and b of Figure 5, respectively. Similar to the case for Nafion and many other PEM materials, the proton conductivity of the composites increases with temperature and relative humidity. This temperature dependence is associated with the thermal activation process of proton conduction, and the influence of humidity on proton transport is presumably due to the water uptake of the membrane and change of ionic domain sizes at different RHs. Furthermore, the NSS composites were found to exhibit higher conductivity than Nafion over the whole range of humidity and temperature measured at 30−90% RH and 30−80 °C, respectively. The activation energy (E_a), the minimum energy required for proton transport across the membrane, was calculated from an Arrhenius plot for proton conductivity (Figure 5b). As given in Table 2, the composite membranes show lower E_a values than bare Nafion, sug-

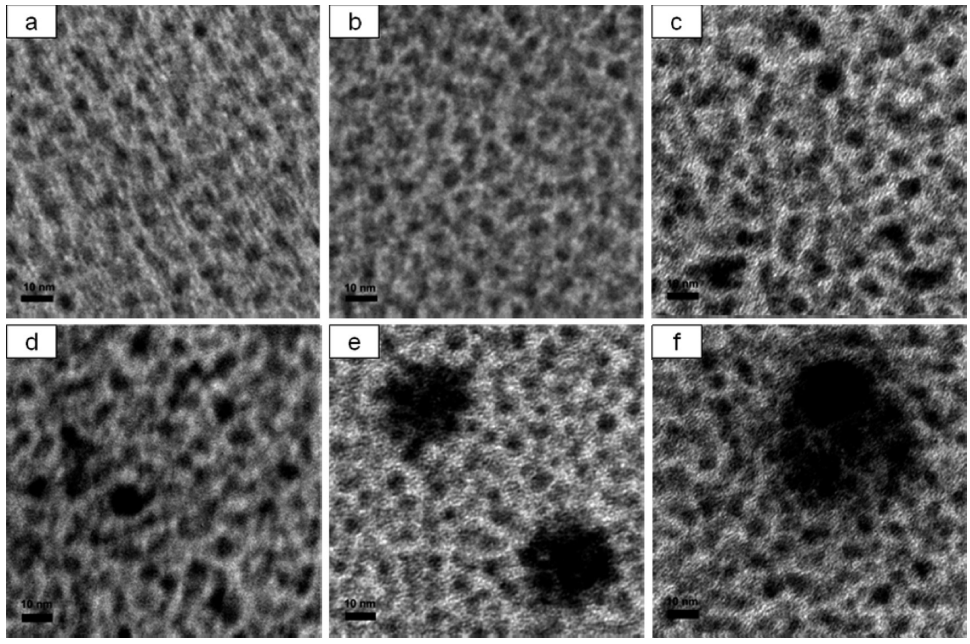

FIGURE 4. Transmission electron micrographs of Nafion/sulfopropylated polysilsesquioxane composite membranes: (a) NSS-0; (b) NSS-4; (c) NSS-8; (d) NSS-12; (e) NSS-16; (f) NSS-20 (the scale bar denotes 10 nm).

Table 1. Characteristics of Nafion/Sulfopropylated Polysilsesquioxane Composite Membranes

membrane	THSPSA content (wt %)	IEC (mmol/g)[a]	water uptake (wt %)[b]	ΔH_f (J/g)[c]	λ[d]
NSS-0	0	0.92 ± 0.02	19.4 ± 0.6	99 ± 2.0	11.7 ± 0.3
NSS-4	4.0	0.99 ± 0.04	21.7 ± 0.6	118 ± 3.0	11.9 ± 0.3
NSS-8	8.0	1.12 ± 0.04	24.9 ± 0.7	121 ± 2.0	12.1 ± 0.3
NSS-12	12.0	1.25 ± 0.04	28.7 ± 0.9	112 ± 2.0	12.8 ± 0.4
NSS-16	16.0	1.29 ± 0.05	29.6 ± 1.0	114 ± 2.0	12.7 ± 0.4
NSS-20	20.0	1.28 ± 0.05	30.2 ± 1.0	114 ± 3.0	13.1 ± 0.4

[a] The ion-exchange capacity (IEC) of the membrane was determined by the titration method. [b] Water uptake at 30 °C in water. [c] The ΔH_f value for bulk water is 334 J/g. [d] Hydration degree, $\lambda = n H_2O/-SO_3H$.

Table 2. Transport Characteristics of Nafion/ Sulfopropylated Polysilsesquioxane Composite Membranes

membrane	proton conductivity (S/cm)[a]	E_a (kJ/mol)	methanol permeability (10^{-7} cm^2/s)[b]	selectivity (10^4)[c]
NSS-0	0.084 ± 0.002	8.7	12.4 ± 0.2	6.8
NSS-4	0.087 ± 0.002	7.4	12.7 ± 0.3	6.9
NSS-8	0.093 ± 0.002	7.4	9.5 ± 0.2	9.8
NSS-12	0.098 ± 0.002	7.0	7.2 ± 0.2	13.7
NSS-16	0.101 ± 0.003	6.7	8.7 ± 0.3	11.7
NSS-20	0.102 ± 0.003	6.8	9.3 ± 0.2	11.0

[a] Proton conductivity measured in liquid water at 30 °C. [b] Methanol permeability measured at 30 °C using 1 M methanol aqueous solution. [c] The selectivity is the ratio of proton conductivity to methanol permeability.

gesting that the proton conduction is more facile in the composites. The decrease of E_a on increasing THSPSA content and IEC value is noteworthy. Undoubtedly, the presence of sulfonic acid side chains in the polysilsequioxane facilitates transport of protons in the membranes. These results are in sharp contrast to those reported for the conventional Nafion/silica composites, where the fillers were found to disrupt the proton diffusion paths and decrease the conductivities (20−22). The observed low E_a values at around 7 kJ/mol imply that conduction at room temperature may occur predominately via the Grotthuss (hopping) mechanism in the NSS composites, which can be idealized as the proton being passed along a chain of rapidly reorienting hydrogen bonds (37). More importantly, as shown in Figure 6, the enhancement in proton conductivity becomes clearly pronounced at high temperatures and low humidity. A conductivity of 0.007 S/cm was determined at 80 °C and 30% RH for NSS-16 and NSS-20 composites, which is more than 2 times greater than that of Nafion. At 120 °C and 30% RH, NSS-16 and NSS-20 membranes yield conductivities of ~0.0102 S/cm, while the conductivity of unfilled Nafion was measured to be around 0.004 S/cm.

To evaluate the potential applications of the prepared composite membranes for DMFCs, the methanol permeability was also studied. It is well-known that an optimum membrane for DMFC application should have high proton conductivity and low methanol crossover (40). Many studies on silica-based composite membranes have revealed that the incorporation of silica particles could reduce methanol crossover by obstructing or winding diffusion pathways for methanol (16−18, 40). However, this decrease in methanol permeability is always accompanied by a reduction in proton conductivity (41). As shown in Table 2, it is important to

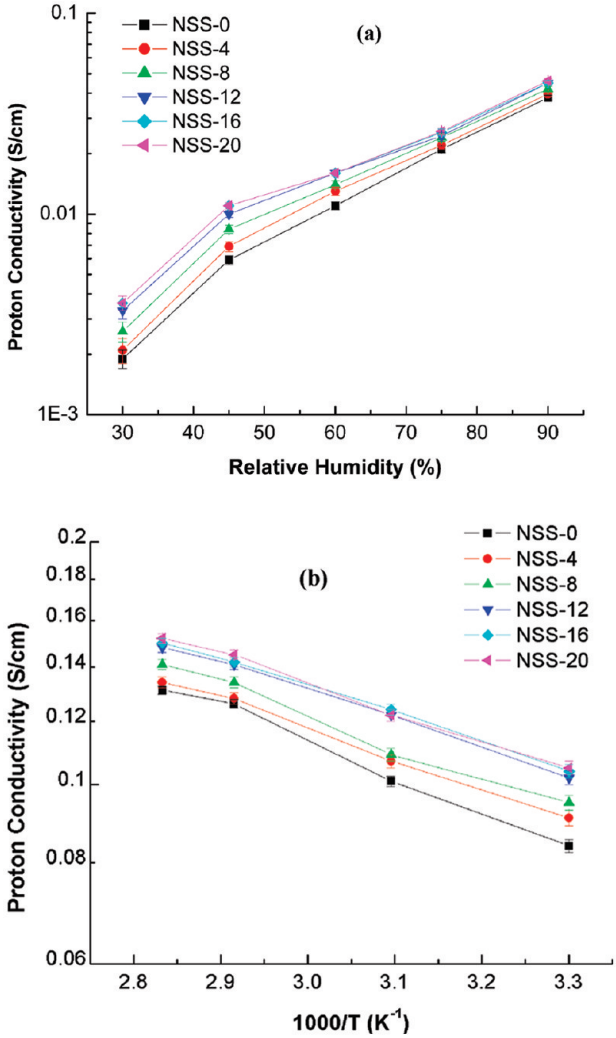

FIGURE 5. (a) Humidity dependence of proton conductivity of the membranes at 30 °C. (b) Temperature dependence of proton conductivity of the membranes under fully hydrated conditions.

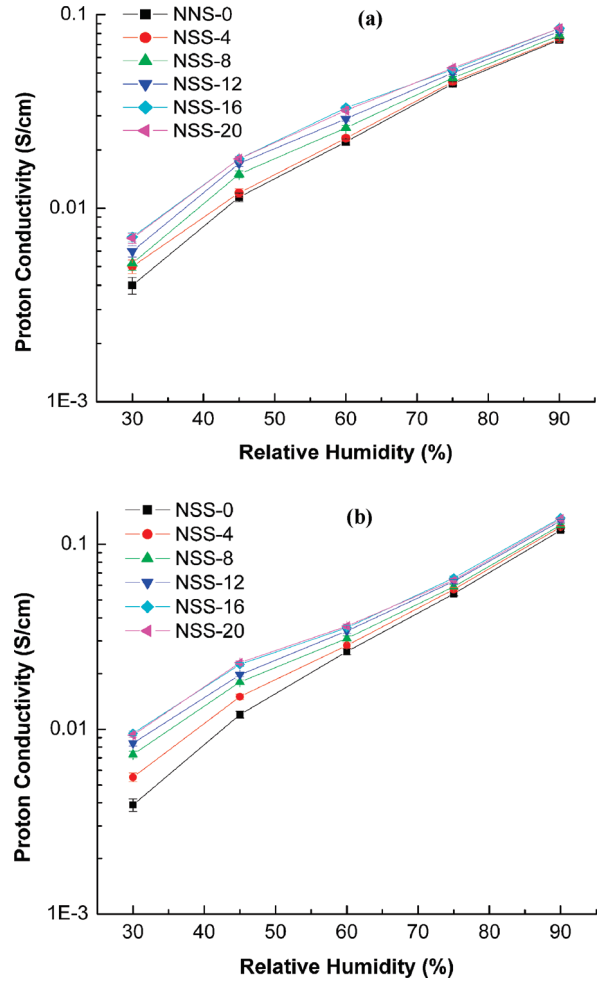

FIGURE 6. Proton conductivity of the composite membranes at (a) 80 °C and (b) 120 °C as a function of relative humidity.

point out that, along with enhanced proton conductivity, the prepared NSS composite membranes containing high THSPSA concentrations (8−20 wt %) also exhibit lower methanol permeability than pristine Nafion. A methanol permeability of 7.15×10^{-7} cm^2/cm was obtained in NSS-12, which is 42% lower than that of plain Nafion. Concurrently, NSS-12 retains a modest improvement in proton conductivity of 17% above Nafion. To capture the vital material parameters important for DMFCs, the electrochemical selectivity, defined as the ratio of proton conductivity to methanol permeability, was calculated and tabulated in Table 2. All of the prepared NSS composite membranes have high selectivities, and in particular, a selectivity of more than 2 times that of Nafion was observed in NSS-12. Generally, an increase in sulfonic acid content and IEC results in a simultaneous increase in both proton conductivity and methanol permeability, thus negating the improvement of selectivity (40). The high selectivities revealed in the prepared membranes are believed to arise from the synergic effect between the polysilsesquioxane and the pendant sulfonic acids. The polysilsesquioxane reduces methanol crossover because of increased tortuosity of hydrophilic domains, while enhanced proton mobility is attributable to the continuous proton-conducting pathways provided by the pendant sulfonic acids.

4. CONCLUSIONS

Novel sol-gel derived Nafion/sulfonated polysilsesquioxane composite membranes have been prepared with varied filler concentrations from a sulfonic acid containing oxide precursor. Membrane properties such as IEC, water uptake, and proton conductivity are strongly related to the concentration of the filler in the composites. In contrast to the conventional Nafion/silica composites, the high content of the sulfonated polysilsesquioxane filler results in higher IEC and water uptake and enables efficient proton conduction. The pendant sulfonic acids on the polysilsesquioxane fillers are believed to promote proton conduction through providing the connectivity of the proton transport channels between the fill and matrix phases in the composite membranes, resulting in proton conductivities higher than those of pristine Nafion over a range of temperatures and relative humidities. More significantly, the prepared composites display conductivity values over 2 times greater than that of unmodified Nafion at high temperatures and low humidity and accordingly less dependence of proton conductivity on humidity. Additionally, these composites are capable of

decreasing methanol permeability without sacrificing the improvement in proton conductivity, leading to superior electrochemical selectivity. This work demonstrates the promising potential of properly modified Nafion composite membranes for applications in elevated-temperature PEMFCs and DMFCs.

Acknowledgment. This work was supported by the National Science Foundation (Grant No. CBET-0932740) and the donors of the Petroleum Research Fund, administered by the American Chemical Society (Grant No. 48373-AC7).

REFERENCES AND NOTES

(1) Appleby, A. J.; Foulkes, R. L. *Fuel Cell Handbook*; Van Nostrand Reinhold: New York, 1989.
(2) Barbir, F. *PEM Fuel Cells: Theory and Practice*; Academic Press: New York, 2005.
(3) Grot, W. G. *Macromol. Symp.* **1994**, 77.
(4) Nakajima, T.; Groult, H. Eds. *Fluorinated Materials for Energy Conversion*; Elsevier: Oxford, U.K., 2005.
(5) Kreuer, K. D. *J. Membr. Sci.* **2002**, *185*, 29.
(6) Sone, Y.; Ekdunge, P.; Simonsson, D. *J. Electrochem. Soc.* **1996**, *143*, 1254.
(7) Paddison, S. J. *Annu. Rev. Mater. Res.* **2003**, *33*, 289.
(8) Zhang, J.; Xie, Z.; Zhang, J.; Tang, Y.; Song, C.; Navessin, T.; Shi, Z.; Song, D. *J. Power Sources* **2006**, *160*, 872.
(9) Li, Q.; He, R.; Jensen, J. O.; Bjerrum, N. J. *Chem. Mater.* **2003**, *15*, 4896.
(10) Jones, D. J.; Roziere, J. *Adv. Polym. Sci.* **2008**, *215*, 219.
(11) Alberti, G.; Casciola, M. *Annu. Rev. Mater. Res.* **2003**, *33*, 129.
(12) Adjemian, K. T.; Lee, S. J.; Srinivasan, S.; Benziger, J.; Bocarsly, A. B. *J. Electrochem. Soc.* **2002**, *149*, A256.
(13) Adjemian, K. T.; Srinivasan, S.; Benziger, J.; Bocarsly, A. B. *J. Power Sources* **2002**, *109*, 356.
(14) Watanabe, M.; Uchida, H.; Emori, M. *J. Phys. Chem. B* **1998**, *102*, 3129.
(15) Zhou, X. Y.; Weston, J.; Chalkova, E.; Hofmann, M. A.; Ambler, C. M.; Allcock, H. R.; Lvov, S. N. *Electrochim. Acta* **2003**, *48*, 2173.
(16) Jiang, R.; Kunz, H. R.; Fenton, J. M. *J. Membr. Sci.* **2006**, *272*, 116.
(17) Antonucci, P. L.; Aricò, A. S.; Cretì, P.; Ramunni, E.; Antonucci, V. *Solid State Ionics* **1999**, *125*, 431.
(18) Miyake, N.; Wainright, J. S.; Savinell, R. F. *J. Electrochem. Soc.* **2001**, *148*, A905.
(19) Guraua, B.; Smotkin, E. S. *J. Power Sources* **2002**, *112*, 339.
(20) Miyake, N.; Wainright, J. S.; Savinell, R. F. *J. Electrochem. Soc.* **2001**, *148*, A898.
(21) Rodgers, M. P.; Shi, Z.; Holdcroft, S. *J. Membr. Sci.* **2008**, *325*, 346.
(22) Damay, F.; Klein, L. C. *Solid State Ionics* **2003**, *162*, 261.
(23) Malhotra, S.; Datta, R. *J. Electrochem. Soc.* **1997**, *144*, L23.
(24) Tazi, B.; Savadogo, O. *Electrochim. Acta* **2000**, *45*, 4329.
(25) Rhee, C. H.; Kim, H. K.; Chang, H.; Lee, J. S. *Chem. Mater.* **2005**, *17*, 1691.
(26) Navarra, M. A.; Croce, F.; Scrosati, B. *J. Mater. Chem.* **2007**, *17*, 3210.
(27) Wang, H.; Holmberg, B. A.; Huang, L.; Wang, Z.; Mitra, A.; Norbeck, J. M.; Yan, Y. *J. Mater. Chem.* **2002**, *12*, 834.
(28) Li, S.; Sun, G.; Ren, S.; Liu, J.; Wang, Q.; Wu, Z.; Sun, H.; Jin, W. *J. Membr. Sci.* **2006**, *272*, 50.
(29) Peraira, F.; Vallé, K.; Belleville, P.; Morin, A.; Lambert, S.; Sanchez, C. *Chem. Mater.* **2008**, *20*, 1710.
(30) Yen, C. Y.; Lee, C. H.; Lin, Y. F.; Lin, H. L.; Hsiao, Y. H.; Liao, S. H.; Chuang, C. Y.; Ma, C. C. M. *J. Power Source* **2007**, *173*, 36.
(31) Rhee, C. H.; Kim, Y.; Lee, J. S.; Kim, H. K.; Chang, H. *J. Power Sources* **2006**, *159*, 1015.
(32) Miyatake, K.; Tombe, T.; Chikashige, Y.; Uchida, H.; Watanabe, M. *Angew. Chem., Int. Ed.* **2007**, *46*, 6646.
(33) Mauritz, K. A.; Warren, R. M. *Macromolecules* **1989**, *22*, 1730.
(34) Mauritz, K. A.; Stefanithis, I. D.; Davis, S. V.; Scheetz, R. W.; Pope, R. K.; Wilkes, G. L.; Huang, H. H. *J. Appl. Polym. Sci.* **1995**, *55*, 181.
(35) Hickner, M. A.; Fujimoto, C. H.; Cornelius, C. J. *Polymer* **2006**, *47*, 4238.
(36) Siu, A.; Schmeisser, J.; Holdcroft, S. *J. Phys. Chem. B* **2006**, *110*, 6072.
(37) Mauritz, K. A.; Moore, R. B. *Chem. Rev.* **2004**, *104*, 4535.
(38) Schmidt-Rohr, K.; Chen, Q. *Nature Mater.* **2008**, *7*, 75.
(39) Jung, D. H.; Cho, S. Y.; Peck, D. H.; Shin, D. R.; Kim, J. S. *J. Power Sources* **2002**, *106*, 173.
(40) Deluca, N. W.; Elabd, Y. A. *J. Polym. Sci. B: Polym. Phys.* **2006**, *44*, 2201.
(41) Li, X.; Roberts, E. P. L.; Holmes, S. M. *J. Power Sources* **2006**, *154*, 115.
(42) Xu, K.; Li, K.; Khanchaitit, P.; Wang, Q. *Chem. Mater.* **2007**, *19*, 5937.

AM900498U